Title
A STUDY OF Dy(40Ar,xn)Po REACTIONS.

Authors
Sikkeland, T.
Silva, R.J.
Ghiorso, A.
et al.

Publication Date
1969-09-01

Submitted to Physical Review

UCRL-18674
Preprint

ey 2

A STUDY OF Dy(^{40}Ar, xn)Po REACTIONS

T. Sikkeland, R. J. Silva,
A. Ghiorso, and M. J. Nurmia

September 1969

AEC Contract No. W-7405-eng-48

LAWRENCE RADIATION LABORATORY
UNIVERSITY of CALIFORNIA BERKELEY

UCRL-18674

ey 2

DISCLAIMER

UCRL-18674

A STUDY OF Dy(^{40}Ar,xn)Po REACTIONS*

T. Sikkeland,† R. J. Silva,‡ A. Ghiorso, and M. J. Nurmia

Lawrence Radiation Laboratory
University of California
Berkeley, California

September 1969

ABSTRACT

Cross sections have been measured for the production of Po nuclides with mass numbers 194 to 200 in bombardments of a 92.7% ^{164}Dy target with ^{40}Ar ions in the ion energy range 160 to 280 MeV. The maximum cross sections (in millibarns) were 0.5, 2.1, 8.0, 35, 50, 70, and 20 for the production of mass numbers 194, 195, 196, 197, 198, 199, and 200, respectively. Isomer ratios for the odd-A nuclides were obtained. A good fit is obtained between the shapes of calculated and experimental excitation function curves. The fit involved (a) calculation of the compound nucleus cross section by the use of the parabolic approximation to the real part of the optical-model potential with the parameters V_o = -70 MeV, r_o = 1.26 F, and d = 0.44 F; (b) modification of Jackson's formula for the probability for neutron emission to include angular momentum effects using T = 1.2 MeV and $\Im/\Im^o$ = 1.4; and (c) assumption of an energy independence for the average partial-level width for neutron emission. In the fitting process experimental values for the latter quantity are obtained to which an empirical formula is fitted. Fission is the main competing mode of decay.

*This work was performed under the auspices of the U.S. Atomic Energy Commission.

†Present address: Norsk Hydro's Institute for Cancer Research, Oslo, Norway (leave of absence).

‡Present address: Oak Ridge National Laboratory, Oak Ridge, Tennessee.

I. INTRODUCTION

The possible existence of a neutron shell at N = 184 and a proton shell at Z = 114 or 126[1] presents an exciting challenge to produce and identify nuclides in that region of the periodic table. One approach is to use (I,xn) reactions which are characterized by the fusion of a heavy ion (I) with a target nucleus (T) to form a compound nucleus (CN) followed by the emission of x neutrons. The ion energy at which a peak occurs in the excitation function depends on the number x, and can therefore be used for mass assignments.

Today the heaviest target available in reasonable quantities is curium (Z_T = 96). The production of superheavy nuclides by (I,xn) reactions depends therefore on whether such reactions take place in this region with ions at least as heavy as Ar (Z_I = 18).

An analysis of the experimental angular-correlation function for coincident fission-fragment pairs gave evidence for the formation of a CN with Z = 110 for the system $^{238}U(^{40}Ar,f)$.[2] However, direct proof for (I,xn) reactions for this system was not furnished. Such reactions have been shown to take place only with ions as heavy as Ne incident on heavy-element targets.[3]

Inspection of the Table of Isotopes[4] reveals that isotopes of Po (Z = 84) are just about the heaviest known nuclides that might be produced with ^{40}Ar as projectile. In this work we chose to investigate in some detail the system $^{164}Dy(^{40}Ar,xn)^{204-x}Po$. Even though Po (Z = 84) is far from Z = 114, it was felt that an analysis of this system was an important step. If the cross sections are forbiddingly small for this system, one cannot hope to produce the superheavy nuclei by this scheme.

The system chosen has several advantages. The product nuclides are known alpha emitters and there are no interfering alpha or EC decay activities

from daughter products or from nuclides produced directly in (^{40}Ar;xn,yp) reactions. Here we have the possibility of studying reactions that involve a wide range both in x and in excitation energy. This provides a stringent test of the validity of the formulas to be used in fitting the experimental data.

II. EXPERIMENTAL

The following two types of experiments were performed: the relative cross sections were determined for the production of the different Po nuclides; and the absolute cross section for the production of ^{200}Po and its recoil range distributions in Al and Ni were determined.

In both types, beams of 415-MeV ^{40}Ar from the Berkeley Hilac were, after magnetic deflection through 30 deg, degraded to the desired energy by the use of weighed Al foils placed in front of the target. The energy resolution of the Ar beam, after passing through the targets and Al foils, was measured by the use of a diffused-junction Si detector. The measured most probable energy is believed to be accurate to within 4 MeV. The beam was collimated to a diameter of 0.6 cm. The average beam current was about 5×10^{-8} A, assuming ^{40}Ar to be fully stripped over the energies considered.

III. EXPERIMENTAL RESULTS

A. Experiments with the Gas Jet

The relative cross sections at various Ar ion energies were determined by the use of the recoil gas-jet technique as described in Ref. 5. The recoil atoms produced in the bombardment were slowed down in helium contained inside a cylindrical chamber 2.5 cm in diameter. To accommodate the longer recoil ranges with ^{40}Ar, the chamber was made 15 cm long; this is to be compared with 4.4 cm, found to be sufficient in experiments with C and O ions.[5]

The recoil collection efficiency of this gas-jet system at various bombarding energies was optimized by adjusting the helium pressure over a range from about 0 to 2 atmospheres. The dysprosium targets, made by electrodeposition onto a 2.1-mg/cm^2 Ni foil, were about 0.5 mg Dy per cm^2 thick. The mass number composition in atom percent of Dy was as follows: 92.7% of 164; 5.55% of 163; 134% of 162; and 0.4% of 161.

The various alpha activities observed could all be assigned to known Po nuclides. A summary of the best decay characteristics, as taken from Ref. 6, is given in Table I. (In the cases where no data were available, we have assumed the alpha branching to be 100%.) As is seen, the odd-A isotopes have a low-spin ground state and a high-spin isomer, and both were produced. The relative yields of the activities were measured at various argon ion energies. After correction for errors due to counting statistics, the yield at a particular bombarding energy was reproducible to within ± 25%. Variations are caused by inhomogeneities in the thickness of the electroplated target combined with variation in the intensity of the beam in the vertical plane and, most important, changes in the collection efficiency of the gas jet.

B. Experiments with Stacked Foils

The experiments with the gas jet showed that the cross sections for ^{164}Dy(^{40}Ar,xn) reactions are negligible when $x \lesssim 3$. Hence, in the bombardment of a ^{nat}Dy target, which consists of ^{164}Dy and lighter isotopes, the 11.4-min alpha activity from ^{200}Po should be the longest-lived component. We therefore decided to use a target of metallic ^{nat}Dy which could be made very uniform by sputtering onto a 0.1-mil Ni backing.

Absolute cross sections and recoil ranges were measured by the use of the stacked-foil recoil catcher technique. Here, a set of Al or Ni foils was

placed directly behind the target, in vacuum. After bombardment, the foils were individually counted for gross alpha decay in 50%-geometry alpha counters. The slowness of this technique limits its use only to those alpha activities for which the half-lives are longer than seconds. Furthermore, only alpha activities which could be identified by their half-lives could be considered.

The bombardments were performed at an Ar ion energy of 172 MeV, giving the maximum yield of ^{200}Po. The gross alpha curve for the various foils in the stack showed, as expected, that the longest-lived component had a half-life of 11.4 min, corresponding to that of ^{200}Po. The distributions of this activity in Al and Ni, along the beam axis, were very nearly Gaussian. The average ranges were 1.40 mg Al per cm^2 and 1.50 mg Ni per cm^2 when a target with a thickness of 0.5 mg ^{nat}Dy per cm^2 was used. After correction for target thickness, the average ranges were found to be 1.6 ± 0.1 mg Al per cm^2 and 1.7 ± 0.1 mg Ni per cm^2. The maximum value of the cross section for the reaction ^{164}Dy(^{40}Ar,4n)^{200}Po was 22 ± 4 mb, assuming 12% alpha branching for ^{200}Po and 23.2% abundance of ^{164}Dy in ^{nat}Dy.

C. Experimental Excitation Functions

The absolute yield of the gas jet at 172 MeV was computed from the relative and absolute production cross sections of ^{200}Po as obtained, respectively, with the gas jet and the stacked-foil technique. By assuming this yield to be independent of bombarding energy, all the measured values for the relative cross section could be converted to absolute cross sections. The latter are given in Table II. Here we have listed the cross sections for the production of the high-spin state σ_A^m, the low-spin state σ_A^g, and their sum σ_A. In Figs. 1 through 6, values for the quantity σ_A, which represents the total cross

section for the production of mass number A, are plotted versus the argon ion bombarding energy. We have not plotted those for A = 194, as the activity of ^{194}Po was below the detection efficiency of the system over most of the energy range.

The data in Table II have not been corrected for effects due to the energy spread in the incident ^{40}Ar beam. The full width at half maximum of this straggling was 9 MeV at 170 MeV and 7 MeV at 260 MeV. As seen from Fig. 1, the FWHM of the measured excitation functions is significantly larger than 9 MeV. The narrowest has a FWHM of 15 ± 4 MeV, which, when corrected for the energy spread, reduces to 12 ± 4 MeV. In addition to statistical errors, an error of 25% is assigned to all the values for the cross section, as mentioned earlier. We have not included errors in the assumed value of 100% for the unmeasured alpha branching rations. Any deviation here will increase the values of the cross sections.

Another possible systematic error is contained in the value used for the absolute yield of the gas jet. Since ^{200}Po is essentially observed only in the ion energy range 165 to 180 MeV, we could not directly check that yield at higher energies. One would expect the yield to decrease with increasing energy as a result of increasing range straggling in helium and a subsequent increase in the loss of recoils to the walls of the chamber. Hence, the cross-section values for the production of the lighter Po isotopes given in Table II must be regarded as lower limits.

IV. DISCUSSION

In the following, the values obtained experimentally for the range and the cross sections are compared with those predicted by the compound-nucleus (CN) mode. According to this model the first step in the process is

characterized by the formation of a CN in a complete fusion of ion and target nuclei. After thermal equilibrium, this nucleus decays by evaporation of neutrons in competition with charged-particle-, γ-ray emission, and fission.

A. The Average Range of ^{200}Po in Al and Ni

A necessary condition for a CN reaction is that the Cn receive the full linear momentum of the ion. Furthermore, since this nucleus, after thermal equilibrium, has lost the memory of its formation, the neutrons are emitted symmetrically around 90 deg in the center-of-mass system of the recoiling nucleus. For a good approximation, the average laboratory-system energy of the nucleus at the end of the cascade of neutrons is $E_R = (m_I m_R / m_{CN}^2) E_I$, where m_I, m_R, and m_{CN} are the masses of the ion, the recoil nucleus, and the compound nucleus, respectively, and E_I is the lab energy of the bombarding ion. Hence, at an ^{40}Ar energy of 172 MeV, the energy of ^{200}Po is 33.1 MeV. This energy corresponds to a velocity of 5.6×10^8 cm/sec. According to Bohr,[7] for velocities greater than the velocity of the electron in the hydrogen atom ($v_o = 2.2 \times 10^8$ cm/sec), the stopping is by electronic interactions; for $V < v_o$, the stopping is by atomic collisions. Bohr's formula is valid for $V < v_o$ and, therefore, cannot be applied. Using his formula, we estimate the ranges to be 2.8 mg Al per cm^2 and 3.4 mg Ni per cm^2--larger than are observed.

Steward and Wallace[8] have developed semi-empirical formulas for the range-energy relationship for particles of various mass and velocity in solids. According to their calculations, ^{200}Po of an energy of 33.1 MeV should have the ranges 1.7 mg/cm^2 and 1.8 mg/cm^2 in Al and Ni, respectively, in good agreement with our experimental results. This agreement supports the hypothesis that ^{200}Po is formed in a CN reaction.

B. Excitation Functions

We first make a few qualitative remarks regarding the values for the isomer ratio σ_A^m/σ_A^g given in Table II. At all energies this ratio in general is larger than unity. This is to be expected, since the average angular momentum of the compound nucleus generally is larger than the spin of the high-spin isomer. We also observe that this ratio has a tendency to increase with increasing bombarding energy. Again this is expected, since average angular momentum of the nucleus at the end of the neutron cascade (and before γ emission) increases with increasing E_i when x is constant. At the peak of the various excitation functions we find σ_A^m/σ_A^g to be about 3, 9, and 3 for the mass numbers 199, 197, and 195, respectively. This might suggest that the α branching for ^{197g}Po is 30% rather than 100%, as assumed in the cross-section evaluation (see Table I).

Let us now discuss the excitation functions for the production of the various mass numbers of Po. If we taken into account that the target is not monoisotopic, the cross section for the production of a Po nuclide of mass number A, at a particular bombarding energy E_{Ar}, is given by the sum

$$\sigma_A = \sum_{A_t} (f\langle G\rangle^x \sigma_x^o)_{A_t}, \qquad (2)$$

where A_t is the mass number of the target nucleus, f is its fractional abundance, x is the number of neutrons emitted from the compound nucleus with A_t as target to give the product A, $\langle G\rangle$ is the average partial-level width for neutron emission in that cascade, and σ_x^o is the cross section for producing A when only neutron emission is considered. This cross section can be expressed as[9]

$$\sigma_x^o = \sum_{=o}^{CN} \sigma_\ell(E_i) P_x(E^*, \ell). \qquad (3)$$

Here, σ_ℓ is the cross section for the ℓth partial wave, ℓ_{CN} is a cutoff value at which the interactions between the nuclei are assumed to change from the compound-nucleus type to the grazing type, and $P_x(E^*, \ell)$ is the probability for the emission of exactly x neutrons from a compound nucleus of angular momentum ℓ and excitation energy E^*. A detailed definition of the quantities used in Eq. (3) is given in Ref. 9.

The calculation of σ_x^o, in 2-MeV intervals of E_i, was performed on a CDC 6600 computer. Values for the particle binding energies, fission barriers, and masses were taken from Ref. 10. For the optical parameters V_o, r_o, and d we used the empirical values -70 MeV, 1.26 F, and 0.44 F, respectively, as obtained in the analysis of the $^{238}U(^{40}Ar,f)$ excitation function.[2]

Best fit was then obtained by using 1.2 MeV for T (the nuclear temperature), 1.4 for $\Im/\Im^o$ (ratio of the effective moment of inertia of the average nucleus in the cascade to that of a rigid spherical nucleus), and the values for $\langle G \rangle$ as given in column 4 of Table III.

The results of the fit are shown in Figs. 1 through 6 where the calculated curves for σ_A are seen to follow the experimental points quite well. We have also shown the contributions from the various target nuclides. Here we see that the yields of ^{200}Po and ^{199}Po are essentially due to ^{164}Dy only. The lighter Dy isotopes contribute significantly only to the front edge of the other excitation-function curves.

The errors in T and $\Im/\Im^o$ are 0.2 MeV and 0.2, respectively. The errors in $\langle G \rangle$ for the systems involving ^{164}Dy are listed in Table III, for

which we took into account the experimental errors in σ_A and the errors in the calculated values for σ_x^o. The latter contributions were significant only for $x = 4$, where the error in σ_x^o was at least 50% because this function is strongly affected by the values for the nuclear parameters V_o, r_o, d, and T.

The normalization used to determine $\langle G \rangle$ for the systems with the lighter target nuclides had to be performed in regions where the functions are steep (see Figs. 3 through 6). Here, the errors are large and difficult to estimate and were therefore not included.

C. Partial-Level Width for Neutron Emission

In Table III we have also included the values for $\langle G \rangle$ as obtained for A = 194 and some of those which can be estimated from the relationship

$$\langle G \rangle = \left[G_I^{x_1} \Big/ G_2^{x_2} \right]^{1/(x_1 - x_2)}, \qquad (4)$$

where $\langle G_1 \rangle$ and $\langle G_2 \rangle$ correspond to those for an (I,x_1n) and an (I,x_2n) reaction, respectively. Values obtained from Eq. (4) have the advantage that their errors depend only on the relative errors in σ_A and σ_x^o. In that respect the value derived from the peaks of the 8n and 10n reactions is especially important, since the reactions occur in the high energy region where the absolute yield of the gas-jet system was not determined.

In column 5 of Table III are given the values for the mass number, A_{av}, of the intermediate nucleus halfway along the evaporation chain, and we see that $\langle G \rangle$ decreases as A_{av} decreases. This suggests that neutron emission suffers an increased competition as we proceed toward the lighter Po nuclides.

To get an idea about what these competing modes might be, we have listed in Table III values of the following nuclear quantities, as averaged

over the nuclei in a cascade: (a) the neutron binding energy, $\langle B_n \rangle$; (b) the fission barrier, $\langle B_f \rangle$; (c) the effective barriers against alpha emission, $\langle B_\alpha \rangle$; and (d) that against proton emission, $\langle B_p \rangle$. The values of the latter two quantities were estimated in the usual way from the sum of the coulomb barrier and the binding energy. Values for the fission barrier and the binding energies for neutrons and protons were taken from Ref. 10, and those for the alpha binding energy were taken from Ref. 6.

A comparison of the values $\langle B_n \rangle$, $\langle B_f \rangle$, $\langle B_\alpha \rangle$, and $\langle B_p \rangle$ in Table IV reveals the interesting fact that those for $\langle B_f \rangle$ show the strongest variation with A_{av}. In addition, they are lower than those for charged-particle emission. This suggests that fission is (a) the main reason for the variation of G with A_{av}, and (b) competing more favorably than charge particle emission with neutron emission. Using the constant-temperature level density formula and ignoring charged-particle emission, the average partial level width for neutron emission can be expressed as[11,12]

$$\langle G \rangle = \left(1 + \langle \Gamma_n / \Gamma_f \rangle^{-1}\right)^{-1} , \tag{5}$$

where

$$\left\langle \Gamma_n / \Gamma_f \right\rangle = C A_{av}^{2/3} \left\{ \exp\left(\beta \Delta / x\right) \right\} \left\{ \exp\left[\left(\langle B_f \rangle - \langle B_n \rangle \right) / T \right] \right\} . \tag{6}$$

Here

$\beta = 0$, when x is even,

$= 1$, when x is odd and A_{CN} is even,

$= -1$, when x is odd and A_{CN} is odd;

T = nuclear temperature (the temperature for fission is assumed to be equal that for neutron emission);

$C = (2T/k_o) \exp\left[(1.5/T)(\Delta_f - \Delta_n)\right]$, ($K_o \approx 10$ MeV and Δ_f and Δ_n are the pairing energies at saddle and equilibrium, respectively);

$\Delta = (\Delta_f + \Delta_n)/(2T)$.

Assuming T, Δ_f, and Δ_n to be constants, we obtained a best fit to the experimental $\langle G \rangle$ values with C = 0.0067, Δ = 1.4, and T = 1.6 MeV. The errors in these values are large. The former is accurate only within a factor of 3, and the errors in Δ and T are about 1.4 and 0.8 MeV, respectively.

The calculated "best fit" values for $\langle G \rangle$, as given in the last column of Table III, are seen to be within the suggested errors for the experimental ones.

V. Conclusion

The analysis of the excitation functions for the production of Po nuclides by (^{40}Ar,xn) reactions suggests that these proceed via the compound-nucleus mechanism.

The shapes of the functions are reproduced by using a nuclear temperature, T, of 1.2 MeV and by taking into account angular momentum effects with a value of 1.4 for the ratio $\mathcal{I}/\mathcal{I}^o$. A similar analysis of (I,xn) excitation functions involving lighter ions in the rare earth region gave T = 2.0 MeV and $\mathcal{I}/\mathcal{I}^o$ = 1.5,[9] and in the heavy-element region T = 1.2 MeV and $\mathcal{I}/\mathcal{I}^o$ = 1.25.[12]

The experimental data for $\langle G \rangle$ are reproduced by a formula which ignores charged-particle emission. The value for the parameter C obtained in this fitting process corresponds to Δ_f being lower than Δ_n by as much as 3 MeV, whereas that for Δ suggests Δ_f to be about equal to cr even larger than Δ_n. In the heavy-element region one finds Δ_f to be about 0.5 MeV larger than Δ_n.[12] We must therefore regard the formulas used to estimate $\langle G \rangle$ as purely empirical.

In conclusion, it appears that there is no systematic difference between ^{40}Ar and lighter ions with respect to the mechanism of (I,xn) reactions. Hence, an extrapolation to heavier ions and targets appears to be safe. Barring unexpected nuclear effects, the success of attempts to produce nuclei in the region of the next closed shells will depend on how severe the fission competition is in the neutron cascade; i.e., it will depend on the strength of the shells.

VI. Acknowledgments

We wish to thank D. F. Lebeck for help in the computer calculations and the Hilac crew for excellent beams. One of us (T.S.) expresses his gratitude to the Norwegian Council for Science and the Humanities, Oslo, Norway, for a research grant and to Professor M. Lefort for a pleasant stay at the Institute of Nuclear Physics, Orsay, France.

References

1) H. Meldner, Arkiv for Fysik 36, 593 (1967).

2) T. Sikkeland, Physics Letters, 27B, 277 (1968).

3) I. Brandstetr, V. V. Volkov, F. A. Ermakov et al., Radiokhimiya 5, 706, (1964).

4) C. M. Lederer, J. M. Hollander and I. Perlman, Table of Isotopes, 6th edition, John Wiley and Sons, Inc., New York (1967).

5) A. Ghiorso, T. Sikkeland and M. J. Nurmia, Phys. Rev. Letters 18, 401 (1967).

6) K. Valli, UCRL-17723, Aug. 1967, submitted to 3rd Int. Conf. on Atomic Masses.

7) N. Bohr, Kg. Danske Videnskab. Selskab, Mat.-fys. Medd. 18, No. 8 (1948).

8) P. G. Steward and R. Wallace, Lawrence Radiation Laboratory Report, UCRL-17314, Dec. 1966.

9) T. Sikkeland, Arkiv for Fysik 36, 539 (1967).

10) W. D. Meyers and W. J. Swiatecki, Lawrence Radiation Laboratory Report, UCRL-11980, May 1965.

11) J. R. Huizenga and R. Vandebosch, Nuclear Reactions, ed. by P. M. Endt and P. B. Smith (North-Holland Publishing Company, Amsterdam, 1962).

12) T. Sikkeland, J. Maly and D. F. Lebeck, Phys. Rev. 169, 1000 (1968).

Figure Captions

Fig. 1 Excitation function for the production of ^{200}Po in the ^{40}Ar bombardments of a Dy target which consisted of 92.7% of ^{164}Dy, 5.6% of ^{163}Dy, and 1.3% of ^{162}Dy. The points are experimental and the curve represents values for the function 0.87 σ_4° where σ_4° is the calculated cross section for the reaction $^{164}Dy(^{40}Ar,4n)$ when only neutron emission is assumed to take place.

Fig. 2 Excitation function for the production of ^{199}Po in the ^{40}Ar bombardments of a Dy target with composition as given in the caption for Fig. 1. The points are experimental; the curve represents the function 0.50 σ_5° where σ_5° is the calculated cross section for the reaction $^{164}Dy(^{40}Ar,5n)$ when only neutron emission is assumed to take place.

Fig. 3 Excitation function for the production of ^{198}Po in the ^{40}Ar bombardments of a Dy target with composition as given in the caption for Fig. 1. The points are experimental. The broken lines I and II, and the solid line, represent the functions 0.18 σ_6°, 0.029 σ_5°, and their sum, respectively. Here σ_6° and σ_5° are calculated cross sections for the reactions $^{164}Dy(^{40}Ar,6n)$ and $^{163}Dy(^{40}Ar,5n)$, respectively, when only neutron emission is assumed to take place.

Fig. 4 Excitation function for the production of ^{197}Po in the ^{40}Ar bombardments of a Dy target with composition as given in the caption for Fig. 1. The points are experimental. The broken lines I, II, and III, and the solid line represent, respectively, the functions 0.11 σ_7°, 0.012 σ_6°, 0.0022 σ_5° and their sum. Here, σ_7°, σ_6°, and σ_5° are calculated cross sections for the reactions $^{164}Dy(^{40}Ar,7n)$, $^{163}Dy(^{40}Ar,6n)$ and $^{162}Dy(^{40}Ar,5n)$, respectively, when only neutron emission is assumed to take place.

Fig. 5 Excitation functions for the production of ^{196}Po in the ^{40}Ar bombardments of a Dy target with composition as given in the caption for Fig. 1. The points are experimental. The broken lines I, II, and III and the solid line represent, respectively, the functions 0.020 σ_8°, 0.0067 σ_7°, and 0.00049 σ_6° and their sum. Here σ_8°, σ_7°, and σ_6° are calculated cross sections for the reactions $^{164}Dy(^{40}Ar,8n)$, $^{163}Dy(^{40}Ar,7n)$, and $^{162}Dy(^{40}Ar,6n)$, respectively, when only neutron emission is assumed to take place.

Fig. 6 Excitation function for the production of ^{195}Po in the ^{40}Ar bombardments of a Dy target with composition as given in the caption for Fig. 1. The points are experimental. The broken lines I, II, and III and the solid line represent, respectively, the functions 0.0067 σ_9°, 0.0075 σ_8°, and 0.00023 σ_7° and their sum. Here, σ_9°, σ_8°, and σ_7° are calculated cross sections for the reactions $^{164}Dy(^{40}Ar,9n)$, $^{163}Dy(^{40}Ar,8n)$, and $^{162}Dy(^{40}Ar,7n)$, respectively, when only neutron emission is assumed to take place.

Table I. Summary of the decay characteristics of the nuclides observed in the bombardments of Dy with ^{40}Ar. The data are taken from Ref. 6.

Nuclide	E_α (MeV)	$T_{1/2}$ (sec)	α branching (%)
^{200}Po	5.86	684	12
^{199g}Po	5.95	300	2.7
^{199m}Po	6.05	246	26
^{198}Po	6.18	102	100*
^{197g}Po	6.28	54	100*
^{197m}Po	6.38	25	100*
^{196}Po	6.52	6	100*
^{195g}Po	6.61	3	100*
^{195m}Po	6.70	1.4	100*
^{194}Po	6.85	0.5	100*

*Assumed in the estimation of the experimental cross sections.

Table II. Experimental cross sections σ_{A} in millibarns ($10^{-27}cm^2$) for the production of ^{A}Po nuclides in the bombardment of a Dy target (92.7% 164; 5.55% 163; 1.34% 162; and 0.4% 161) with ^{40}Ar ions. The superscripts, g and m, in the symbol for the cross section symbolize the ground state and high spin isomers, respectively.

E_{Ar} (MeV)	σ_{200}	σ^{g}_{199}	σ^{m}_{199}	σ_{199}	σ_{198}	σ^{g}_{197}	σ^{m}_{197}	σ_{197}	σ_{196}	σ^{g}_{195}	σ^{m}_{195}	σ_{195}	σ_{194}	$\frac{\sigma^{m}_{199}}{\sigma^{g}_{199}}$	$\frac{\sigma^{m}_{197}}{\sigma^{g}_{197}}$	$\frac{\sigma^{m}_{195}}{\sigma^{g}_{195}}$
162	1.9±0.6	0.8±0.3	0.5±0.2	1.3±0.5	0.17±0.06	--	$\leqslant 10^{-2}$	$\leqslant 10^{-2}$						0.63		
172	19±5	8.4±2.1	10±3	18±5	1.2±0.4									1.2		
175	20±5	15±4	24±5	39±10	6.0±1.8	$8\pm8\cdot10^{-3}$	0.3±0.2	0.4±0.2	$\leqslant 2\cdot10^{-2}$					1.6	4.2	
179	9.2±2.3															
182	4.2±1.1	21±5	47±12	68±17	20±5									2.2		
186		13±3	36±9	49±12	25±5	0.24±0.10	2.1±0.7	2.3±0.8	0.11±0.04					2.8	8.7	
193	0.45±0.17															
196		4.2±1.2	13±4	17±4	48±12	1.1±0.3	10±3	11±3	0.43±0.16					3.1	9.1	
203						1.6±0.5	13±3	15±4	1.4±0.4	$4(\pm3)\cdot10^{-2}$	$3(\pm2)\cdot10^{2}$	$7(\pm4)\cdot10^{-2}$			8.1	0.8
207		0.3±0.1	0.6±0.2	0.9±0.3	34±9									2.0		
220		⩽0.3	0.05±0.03	0.05±0.03	2.1±0.6	3.1±0.8	27±7	30±8	8±2	0.09±0.05	0.3±0.1	0.4±0.12			8.7	3.3
225						1.5±0.5	13±4	15±4	8±2	0.16±0.07	0.45±0.17	0.6±0.2			8.7	2.8
232					0.2±0.1	0.6±0.2	7.6±2.5	8.2±2.6	6±2	0.11±0.05	0.64±0.25	0.8±0.3			12	5.8
242						0.2±0.1	3.2±1.1	3.4±1.2	6±2	0.6±0.2	1.5±0.5	2.1±0.7	0.08±0.03		16	2.5
256						0.015±0.010	0.35±0.15	0.37±0.15	1.4±0.5	0.5±0.2	1.4±0.4	1.9±0.6	0.5±0.2		23	2.8
262						0.02±0.01	0.16±0.07	0.18±0.08	1.1±0.4	0.4±0.2	1.4±0.4	1.8±0.6	0.3±0.1		8	3.2
280									0.026±0.014				0.3±0.1			
286							$7\pm7\cdot10^{-3}$		0.05±0.03	0.04±0.02	0.16±0.08	0.2±0.1				4.0

Table III. Results of the analysis of experimental excitation functions for Dy(^{40}Ar,xn)Po reactions. Here A_t is mass number of the target nucleus with an abundance of f%; x is the number of neutrons emitted from the compound nucleus to give ^{A}Po: ⟨G⟩ (exp) is the normalization factor used to obtain a fit to the absolute cross section and represents the average partial level width for neutron emission in the cascade; A_{av} is the mass number of the intermediate nucleus halfway along the cascade; ⟨B⟩, ⟨B_f⟩, ⟨B_n⟩, and ⟨B_p⟩ are the average values for the neutron binding energy, fission barrier, effective barrier for α emission, and effective barrier for proton emission, respectively. In the last column are listed calculated values for ⟨G⟩ as described in the text.

A_t	f (%)	x x_1/x_2	⟨G⟩ (exp)	A_{av}	⟨B_n⟩ (MeV)	⟨B_f⟩ (MeV)	⟨B_α⟩ (MeV)	⟨B_p⟩ (MeV)	⟨G⟩ (calc.)
164	92.7	4	0.98 ±0.25	202.5	8.4	14.2	15.9	15.5	0.90
164	92.7	5	0.89 ±0.05	202	8.6	13.6	15.9	15.3	0.85
164	92.7	6	0.76 ±0.05	201.5	8.5	13.3	15.8	15.0	0.83
164	92.7	7	0.74 ±0.05	201	8.7	12.9	15.8	14.9	0.77
164	92.7	8	0.62 ±0.05	200.5	8.7	12.6	15.8	14.8	0.74
164	92.7	9	0.58 ±0.05	200	8.8	12.2	15.7	14.8	0.66
164	92.7	10	0.52 ±0.05	199.5	8.8	11.9	15.6	14.7	0.63
163	5.6	5	0.88	201	8.7	12.8	15.8	14.9	0.76
163	5.6	6	0.77	200.5	8.7	12.5	15.8	14.8	0.72
163	5.6	7	0.74	200	8.8	12.1	15.7	14.8	0.65
163	5.6	8	0.58	199.5	8.8	11.8	15.6	14.7	0.61
162	1.3	5	0.69	200	8.9	12.0	15.7	14.8	0.62
162	1.3	6	0.58	199.5	8.8	11.7	15.3	14.3	0.59
162	1.3	7	0.57	199	8.9	11.4	15.4	14.4	0.53
		7/5	0.47 ±0.10	198.5	8.9	11.1	15.4	14.5	0.47
		8/6	0.33 ±0.10	197.5	9.0	10.4	15.3	14.3	0.35
		9/7	0.25 ±0.07	196.5	9.1	9.8	15.2	14.1	0.25
		10/8	0.25 ±0.05	195.5	9.2	9.3	15.1	14.1	0.18

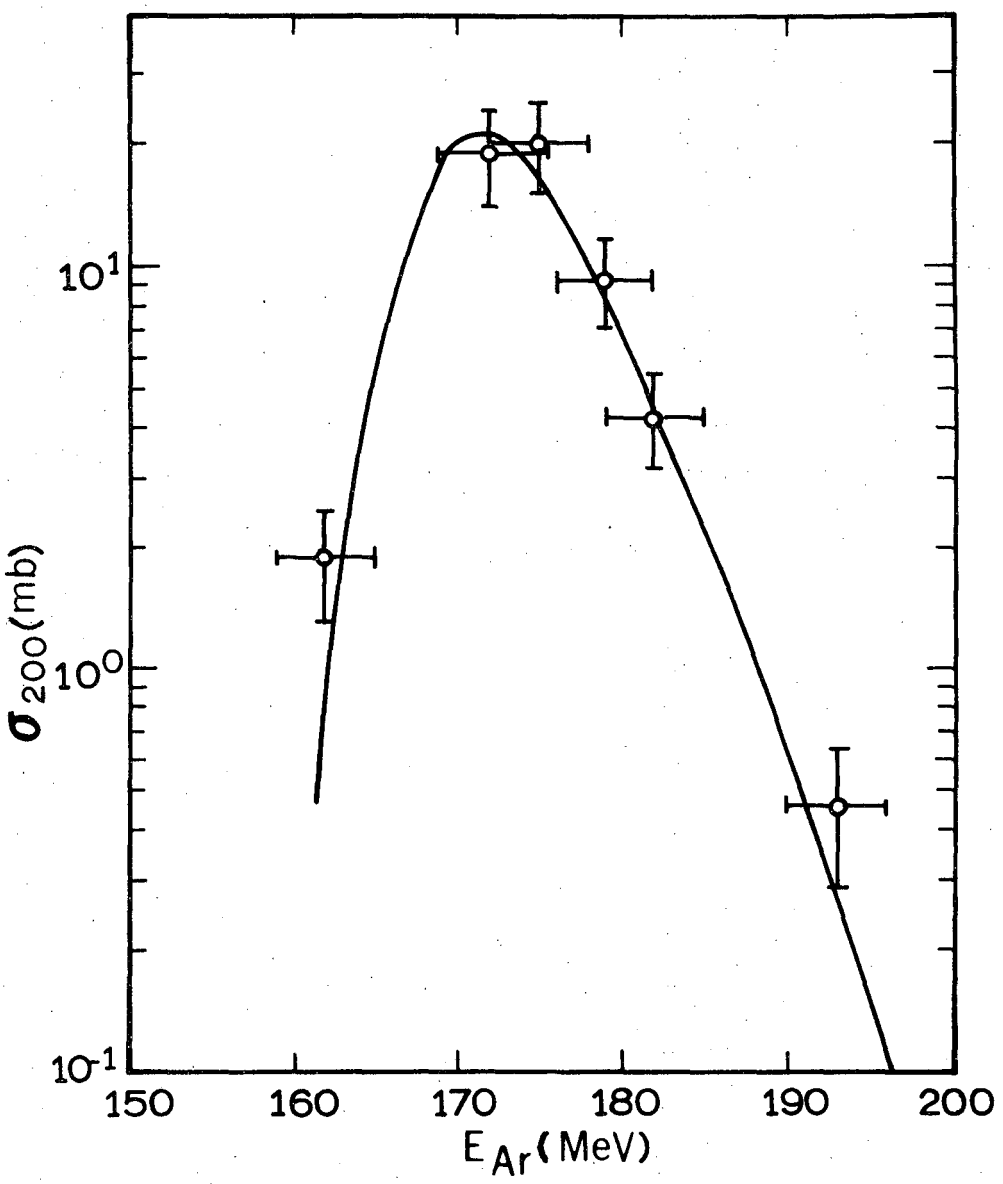

XBL 699 4916

Fig. 1

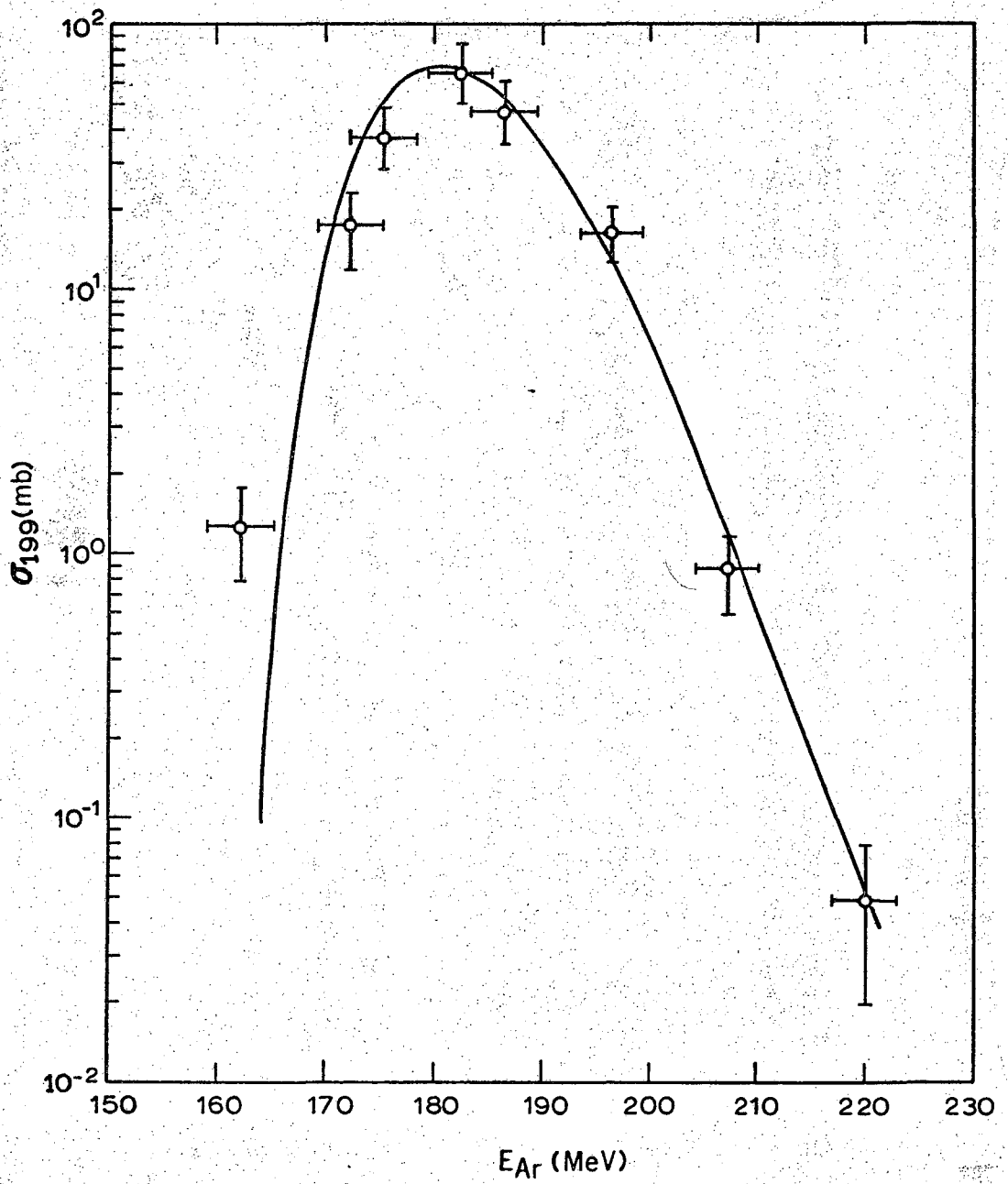
10^2
10^1
10^0
10^{-1}
10^{-2}
σ_{199}(mb)
150
160
170
180
190
200
210
220
230
E_{Ar} (MeV)
XBL 699 4917

Fig. 2

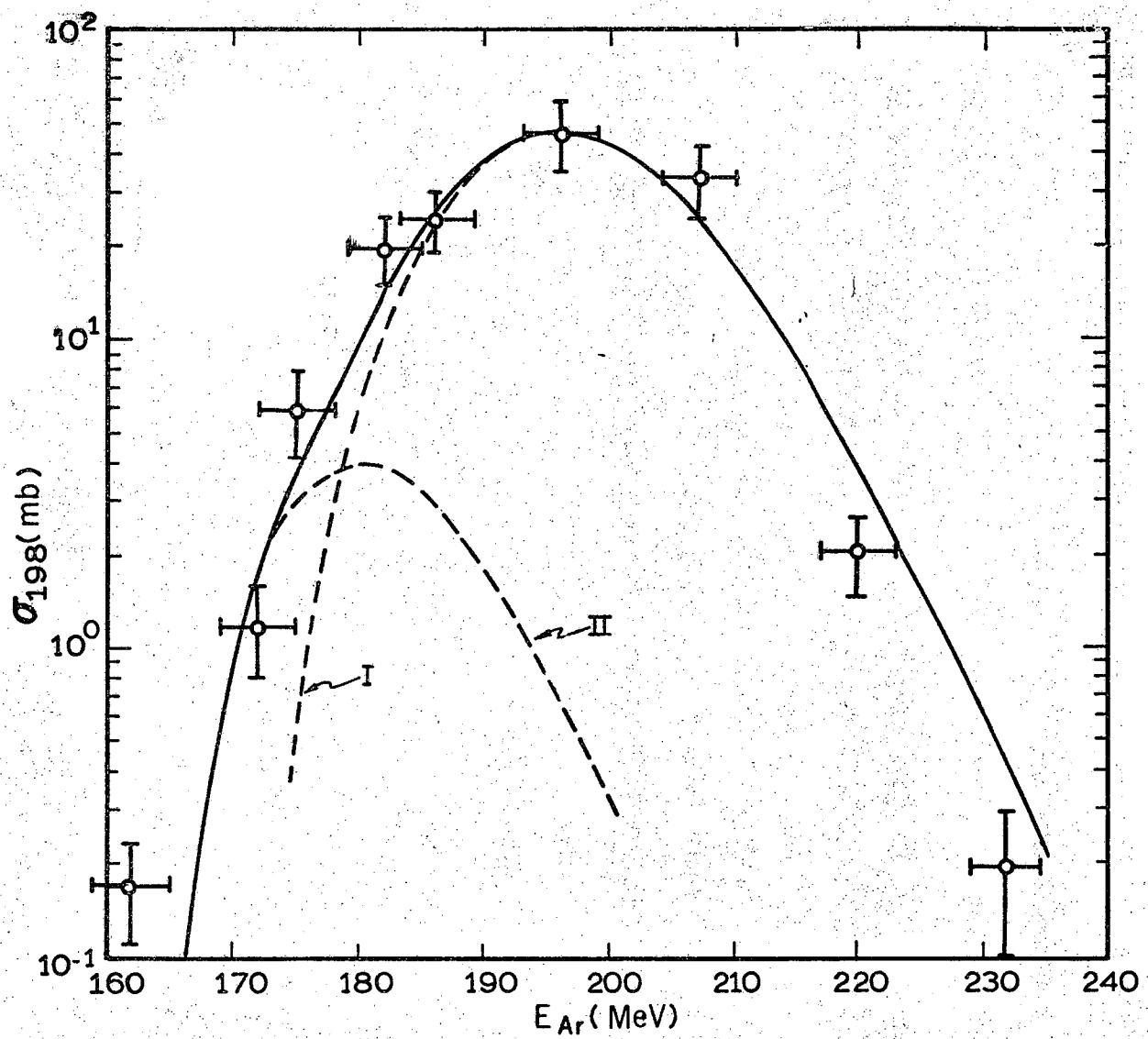

XBL 699 4918

Fig. 3

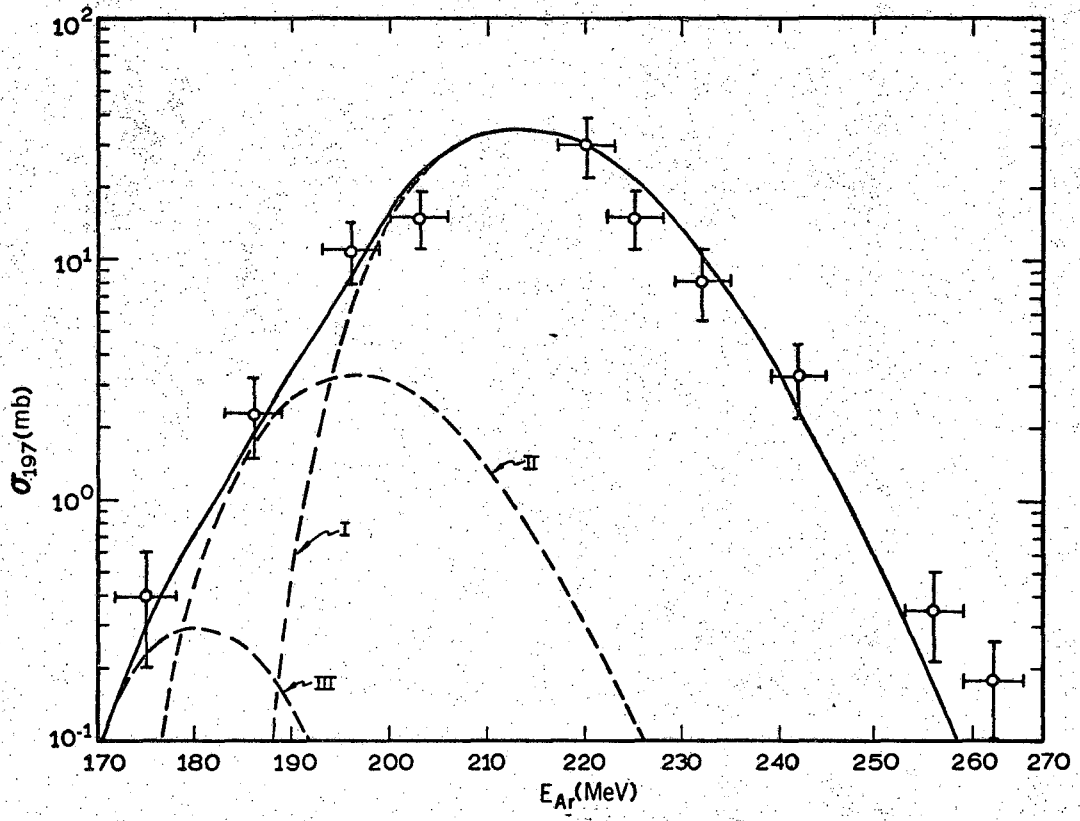

XBL 699 4919

Fig. 4

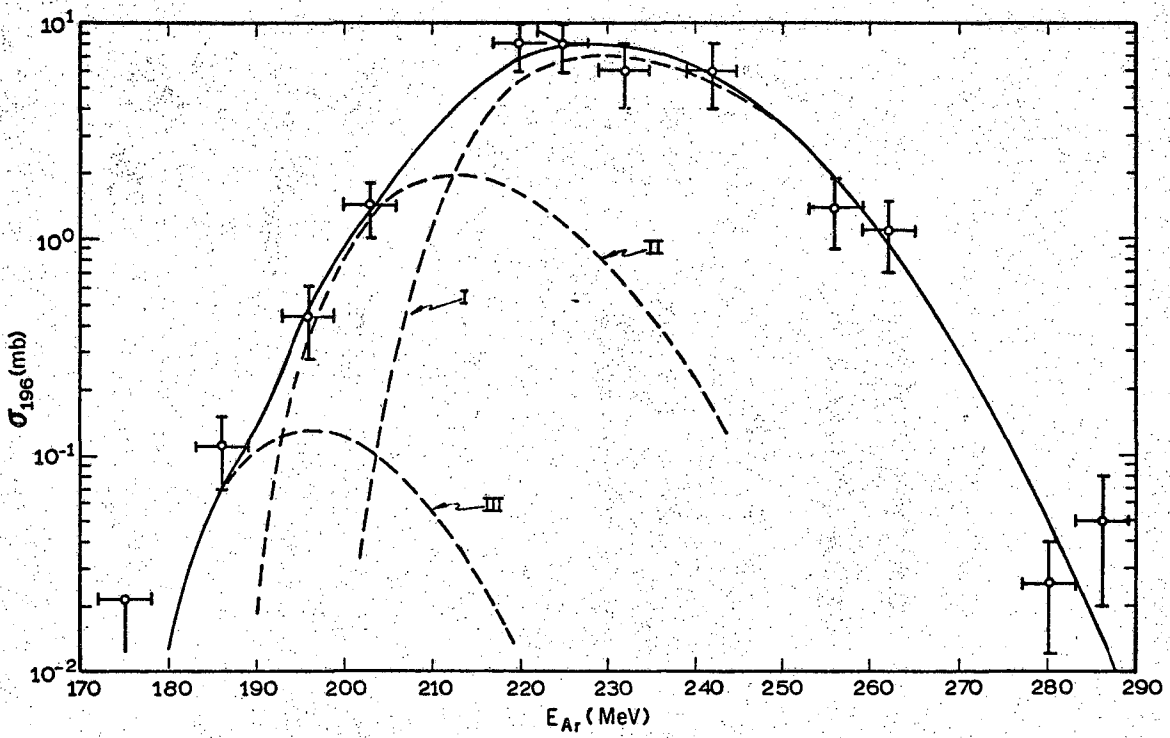

XBL 699 4920

Fig. 5

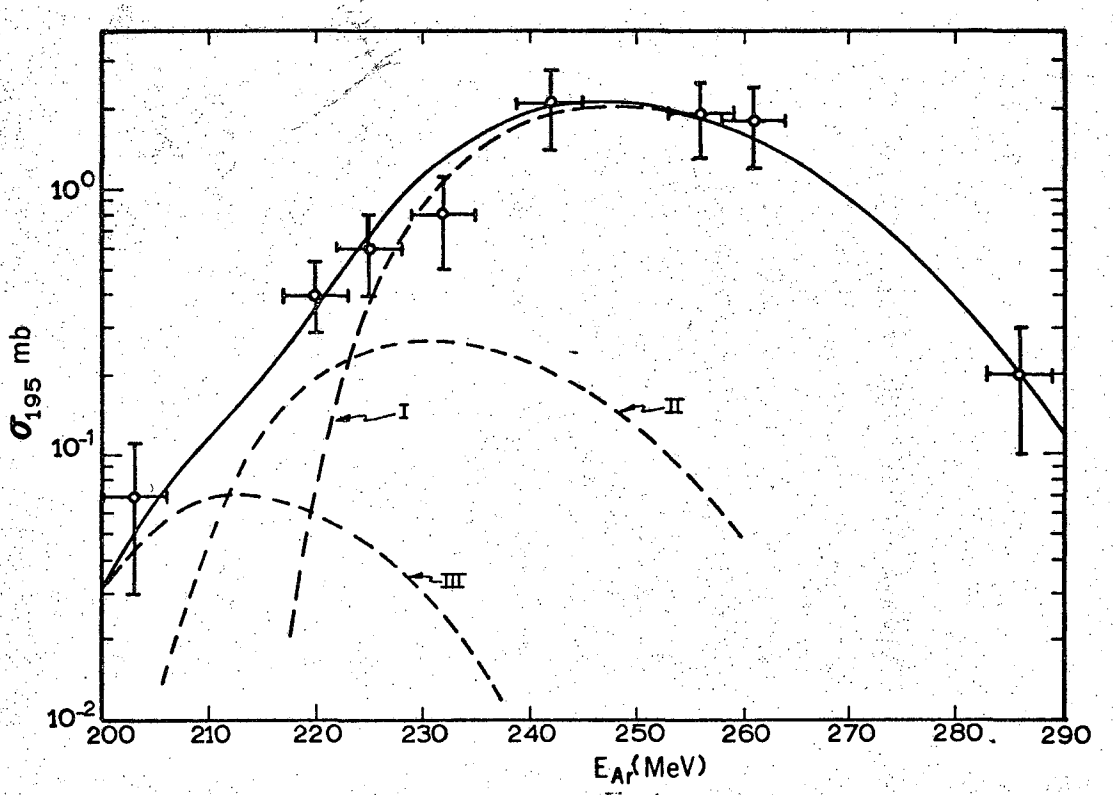

XBL 699 4921

Fig. 6

TECHNICAL INFORMATION DIVISION
LAWRENCE RADIATION LABORATORY
UNIVERSITY OF CALIFORNIA
BERKELEY, CALIFORNIA 94720